

True Structure of Trigonal Bipyramidal SiO_4F^- Species in Siliceous Zeolites

Martin P. Attfield,^{†,‡} C. Richard A. Catlow,^{*,†} and Alexey A. Sokol[†]

Davy-Faraday Research Laboratory, The Royal Institution of Great Britain, 21 Albemarle Street, London, W1S 4BS, UK, and School of Crystallography, Birkbeck College, Malet Street, London, WC1E 7HX, UK

Received May 30, 2001. Revised Manuscript Received August 13, 2001

This paper describes the true geometry of the pentacoordinated SiO_4F^- units found in several all-silica zeolite systems, as determined by ab initio density functional calculations. The SiO_4F^- units in the two zeolites (sodalite and ferrierite) studied contain Si–F bonds of 1.71 and 1.76 Å in length, and all the Si–O bonds in the units are elongated with respect to the Si–O bonds in the tetrahedral SiO_4 unit typically found in a zeolite. All the bond angles in the SiO_4F^- unit agree with those expected for a regular trigonal bipyramidal XY_5 unit. The calculated structure is shown to reproduce accurately an averaged structural model determined by standard crystallographic methods. The approach we have developed in this work has general implications for the solution of complex local structure problems in solids.

Introduction

The introduction of fluoride anions in the syntheses of zeolites has been known for more than 20 years, since the patent report of Flanigen and Patton.¹ The role of the F^- anions in the synthesis is believed to be as a mineralizing agent to enhance the reactivity of silica. The inclusion of the F^- ions into syntheses of aluminosilicates and gallophosphates has also been used to form known and novel microporous structure types, many of which have the F^- ion occluded as part of the framework structure.^{2–5} Within the zeolite area specifically, the use of the fluoride method of synthesis has led to the formation of several pure silica (SiO_2) zeolites⁶ of high crystallinity and low defect concentration.⁷ The fluoride ion is believed to direct the formation of the noncentrosymmetric zeolite IFR,⁸ which has strong nonlinear

optical effects, and the treatment, and possibly incorporation, of the fluoride ion into zeolites has also been shown to produce enhanced acidity of the treated material.⁹ In this paper we apply computational methods to examine the structures of F^- containing microporous silica and show clearly the stability and structure of a *pentacoordinated Si species* whose presence has previously been suggested on the basis of NMR and X-ray diffraction studies, but whose complete structure has not been fully determined.

Pure silica zeolites are generally prepared by heating a gel, containing a SiO_2 source, a structural directing agent (SDA), a mineralizing agent, and a solvent, under hydrothermal conditions. Typically, the SDA is a quaternary ammonium compound, the mineralizing agent is OH^- or F^- ions, and the solvent is water. The resulting solid product contains the SDA within the void volume of the neutral SiO_2 framework. When the SDA is a cationic species, its charge must be compensated by negatively charged species, which are normally the OH^- or F^- ions. The location of the SDA is often well-established within the zeolite as they are large molecules, have a high crystallographic occupancy, are frequently well-ordered, and can often only fit into certain sites within the void space of the zeolite. This is not the case when considering the charge-compensating anions, as they may occupy many different sites and only at a low level of crystallographic occupancy. Much effort has been spent on trying to identify the sites of the charge-compensating anions, which is particularly so for the F^- ion. To date, computational,¹⁰ NMR,^{11–14}

* Corresponding author. E-mail: richard@ri.ac.uk.

[†] The Royal Institution of Great Britain.

[‡] Birkbeck College.

(1) Flanigen, E. M.; Patton R. L. U.S. Patent 4,073,865, 1978.

(2) Delmotte, L.; Souillard, M.; Guth, F.; Seive, A.; Lopez, A.; J. L. *Zeolites* **1990**, *10*, 778.

(3) Estermann, M.; McCusker, L. B.; Baerlocher, C.; Merrouche, A.; Kessler, H. *Nature* **1991**, *352*, 320.

(4) Weigel, S. J.; Weston, S. C.; Cheetham, A. K.; Stucky, G. D. *Chem. Mater.* **1997**, *9*, 1294.

(5) Wragg, D. S.; Bull, I.; Hix, G. B.; Morris, R. E. *J. Chem. Soc. Chem. Commun.* **1999**, 2037.

(6) (a) Guth, J. L.; Kessler, H.; Caultet, H.; Hazm, J.; Merrouche, A.; Patarin, J. *Proceedings 9th International Zeolite Conference*; von Ballmoos, R.; Higgins, J. B.; Treacy, M. M., Eds.; Montreal, 1992. (b) Deforth, U.; Unger, K. K.; Schuth, F. *Microporous Mater.* **1997**, *9*, 287. (c) Kuperman, A.; Nadimi, S.; Oliver, S.; Ozin, G. A.; Garces, J. M.; Olken, M. M. *Nature* **1993**, *365*, 239. (d) Weigel, S. J.; Gabriel, J. C.; Gutierrez Puebla, E.; Monge Bravo, A.; Henson, N. J.; Bull, L. M.; Cheetham, A. K. *J. Am. Chem. Soc.* **1996**, *118*, 2427. (e) Lewis, J. E.; Freyhardt, C. C.; Davis, M. E. *J. Phys. Chem.* **1996**, *100*, 5039. (f) Lindlar, B.; Felsche, J.; Behrens, P.; Van de Goo, G. *J. Chem. Soc. Chem. Commun.* **1995**, 2559. (g) Villaescusa, L. A.; Barrett, P. A.; Cambor, M. A. *Angew. Chem., Int. Ed. Engl.* **1999**, *38*, 1997. (h) Cambor, M. A.; Villaescusa, L. A.; Diaz-Caban, M. J. *Topics in Catalysis* **1999**, *9*, 59.

(7) Axon, S. A.; Klinowski, J. *Applied Catal. A* **1992**, *81*, 27.

(8) Bull, I.; Villaescusa, L. A.; Teat, S. J.; Cambor, M. A.; Wright, P. A.; Lightfoot, P.; Morris, R. E. *J. Am. Chem. Soc.* **2000**, *122*, 7128.

(9) Kowalak, S.; Khodakov, A. Yu.; Kustov, L. M.; Kazansky, V. B. *J. Chem. Soc., Faraday Trans.* **1995**, *91*, 385.

(10) George, A. R.; Catlow, C. R. A. *Zeolites* **1997**, *18*, 67.

(11) Koller, H.; Wolker, A.; Valencia, S.; Villaescusa, L. A.; Diaz-Caban, M. J.; Cambor, M. A. *Proceedings of the 12th International Zeolite Conference*; Treacy, M. M. J., Marcus, B. K., Bisher, M. E., Higgins, J. B., Eds.; Baltimore, 1998.

(12) Koller, H.; Wolker, A.; Villaescusa, L. A.; Diaz-Caban, M. J.; Valencia, S.; Cambor, M. A. *J. Am. Chem. Soc.* **1999**, *121*, 3368.

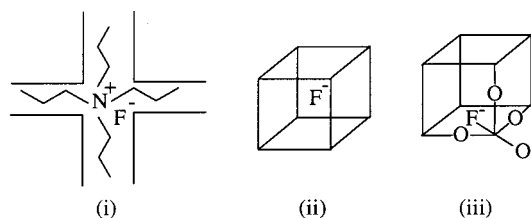


Figure 1. A schematic representation of the three types of F^- ion environments found in siliceous zeolites: (i) as part of an ion pair, (ii) in the center of a small cage far from any Si atoms, and (iii) coordinated to a Si atom to form part of a pentacoordinated SiO_4F^- unit.

and X-ray diffraction methods have all been used to characterize the locations and local structure of the F^- ions in the as-synthesized all-silica zeolites. However, the aforementioned problems of low concentration, disorder, and their change in mobility as a function of temperature makes full structural characterization of the location and environment of the F^- ions very difficult. The results of these studies report three general fluoride environments: (i) the F^- ions reside in close proximity to the positively charged SDA as an ion pair in the main void volume of the zeolite;¹⁵ (ii) the F^- ions are separated far from the SDA and are located centrally within small cages in the framework of the material, but at rather large distances from the closest Si atom;¹⁶ and (iii), as for point (ii), except that the F^- ions are coordinated to a Si atom to form a pentacoordinated SiO_4F^- unit within the small cage.^{8,17} The two latter cases may be related, in that on cooling the material, the F^- ions in environment ii becomes less mobile and adopt the configuration described in case (iii) as for MFI.¹³ However, at room temperature, examples of both environments are known.^{13,18} The three fluoride environments are shown schematically in Figure 1.

The only method by which the spatial arrangement of all three F^- ion environments has been characterized is X-ray diffraction. As far as we are aware, only one example of environment (i) is known, although there is some dispute as to the validity of this structure;^{12,19} three examples of environment (ii) are known,^{16,19,20} and four instances of environment (iii) have been reported.^{8,17,18,21} The SiO_4F^- unit found in iii is of particular interest as it was thought for a long time that 5-coordinate Si in a zeolite did not exist. Only in two of these studies, that on $[\text{Cocp}_2]\text{-F}^-[\text{Si-NON}]$ ¹⁷ and $\text{F}^-[\text{Si-IFR}]$,⁸ has the transformation of the SiO_4 tetrahedral

unit toward a trigonal bipyramidal SiO_4F^- unit with chemically sensible noncontact distances between the O and F atoms been observed. In these studies the Si-F bond length is 1.836 and 1.92 Å for $[\text{Cocp}_2]\text{-F}^-[\text{Si-NON}]$ and $\text{F}^-[\text{Si-IFR}]$, respectively, which is rather long for a typical covalent or ionic Si-F bond length, as seen in SiF_4 or SiF_6^{2-} , where bond lengths of 1.56 and 1.68 Å, respectively, are reported.^{22,23} The Si-F bond lengths observed in other structures containing F^- ions in environment type (iii) are in the range 1.94–1.99 Å. We consider that these values are somewhat large and do not represent the real value of the Si-F bond length. We assume that the overestimation of the Si-F bond length arises from the low crystallographic occupancy of the F^- ion sites in these structures, where the maximum so far is 50%,^{8,17} and the fact that only an averaged structure is obtained from crystallographic methods, making it difficult to obtain the true local structure of the SiO_4F^- units.

In this work, we use ab initio electronic structure techniques to model the incorporation of a fluoride species into all-silica zeolites in order to calculate the true local structure of the SiO_4F^- units. Computational methods provide the only way to determine accurately and unempirically the complete structure of this unit in structures where its concentration is relatively low. Initially, we investigate candidate structures in a simple material, sodalite, whose unit cell is one of the smallest of the zeolite family of materials and which has been extensively used in recent work on the defect formation in zeolites.²⁴ Utilizing our results for the sodalite system, we apply energy minimization to a system based upon an experimentally determined structure of the all-silica zeolite ferrierite that has been found to contain the SiO_4F^- unit. The resulting minimized structure for this ferrierite system is used to generate a single crystal X-ray diffraction data set. The latter is used in a crystallographic structure solution to obtain a structure that is compared directly with the experimentally determined ferrierite structure. Our work shows that by combining ab initio methods with experimental techniques, we acquire a powerful method for determining complex local structures in solids.

Methodology

Computational Details. An energy minimization technique based on an ab initio density functional theory (DFT) approach, as implemented in the DSolid/Dmol³ computational code,²⁵ was employed to obtain the structural data pertaining to the F^- ion encapsulated in the all-silica sodalite and ferrierite zeolite materials. The GGA PW91 exchange and correlation density functionals²⁶ were used along with a double numerical atomic basis set complemented by single polarization functions (DNP) on a medium quality integration grid (program default²⁵) for the geometry optimization.

(13) Koller, H.; Wolker, A.; Eckert, H.; Panz, C.; Behrens, P. *Angew. Chem., Int. Ed. Engl.* **1997**, *36*, 2823.

(14) (a) Fyfe, C. A.; Lewis, A. R.; Chezeau, J. M.; Grondy, H. *J. Am. Chem. Soc.* **1997**, *119*, 12210. (b) Fyfe, C. A.; Brouwer, D. H.; Lewis, A. R.; Chezeau, J. M. *J. Am. Chem. Soc.* **2001**, *123*, 6882.

(15) Price, G. D.; Pluth, J. J.; Smith, J. V.; Bennett, J. M.; Patton, R. L. *J. Am. Chem. Soc.* **1982**, *104*, 5971.

(16) Caullet, P.; Guth, J. L.; Hazm, J.; Lamblin, J. M.; Gies, H. *Eur. J. Solid State Inorg. Chem.* **1991**, *28*, 345.

(17) van de Goor, G.; Freyhardt, C.; Behrens, P. *Z. Anorg. Allg. Chem.* **1995**, *621*, 311.

(18) (a) Attfield, M. P. PhD thesis, UCSB, 1996. (b) Attfield, M. P.; Weigel, S. J.; Taulelle, F.; Cheetham, A. K. *J. Chem. Mater.* **2000**, *10*, 2109.

(19) Mentzen, B. F.; Sacerdote-Peronnet, M.; Guth, J. L.; Kessler, H. *C. R. Acad. Sci. Paris Ser. II* **1991**, *313*, 177.

(20) Barrett, P. A.; Cambor, M. A.; Corma, A.; Jones, R. H.; Villaescusa, L. A. *J. Phys. Chem. B* **1998**, *102*, 4147.

(21) Cambor, M. A.; Diaz-Cabanas, M.-J.; Perez-Pariente, J.; Teat, S. J.; Clegg, W.; Shannon, I. J.; Lightfoot, P.; Wright, P. A.; Morris, R. E. *Angew. Chem. Int. Ed.* **1998**, *37*, 2122.

(22) *CRC Handbook of Chemistry and Physics*, 75th ed.; Lide, D. R., Ed.; CRC Press Inc.: Boca Raton, FL, 1994.

(23) Loehlin, J. H. *Acta Crystallogr. B* **1993**, *49*, 967.

(24) Attfield, M. P.; Catlow, C. R. A.; Sokol, A. A. Manuscript in preparation.

(25) (a) Delley, B. *J. Chem. Phys.* **1990**, *92*, 508. (b) *EOM DSolid User Guide*; Molecular Simulations, Inc.: San Diego, 1996. (c) *Dmol³, Cerius² 3.5, User Guide*; Molecular Simulations, Inc.: San Diego, CA, 1997.

(26) (a) Perdew, J. P.; Zunger, A. *Phys. Rev. B* **1981**, *23*, 5048. (b) Perdew, J. P.; Wang, Y. *Phys. Rev. B* **1989**, *40*, 3399. (c) Perdew, J. P.; Wang, Y. *Phys. Rev. B* **1992**, *45*, 13244.

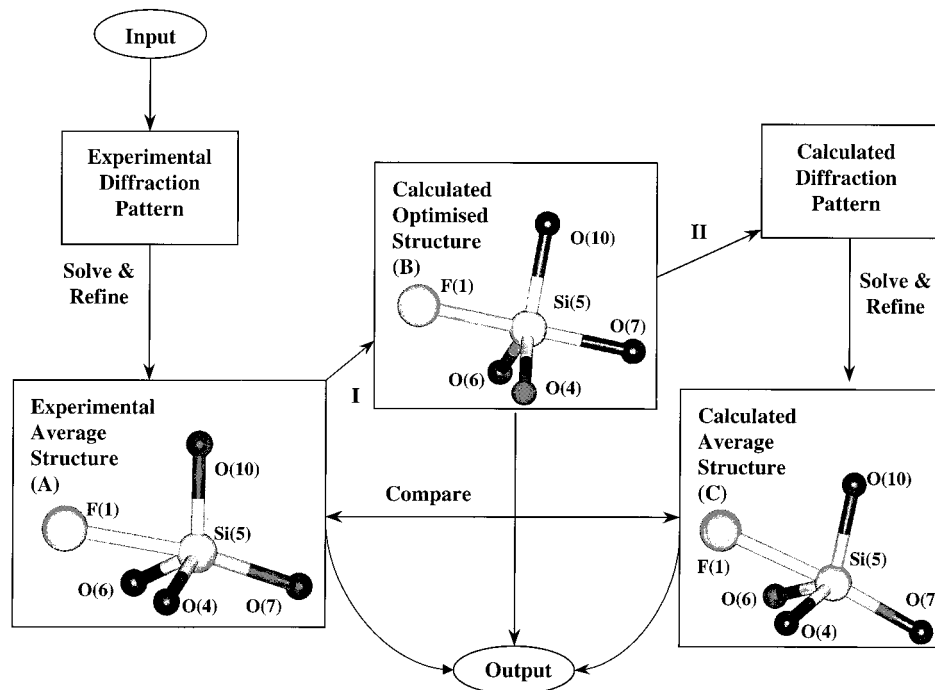


Figure 2. Steps for determination of the local structure SiO_4F^- unit in the zeolite ferrierite produced by a combination of computational and crystallographic methods. The actual structures of the SiO_4F^- unit for (A) $\text{Cu}_{0.964}\text{F}_{1.2}(\text{Si}_{36}\text{O}_{72})\cdot 4\text{C}_5\text{H}_5\text{N}^{18}$ (space group $Pm\bar{m}n$), (B) $\text{KF}(\text{Si}_{36}\text{O}_{72})\cdot 4\text{C}_5\text{H}_5\text{N}$ (space group $P1$), and (C) $\text{F}_{1.02(2)}(\text{Si}_{36}\text{O}_{72})$ (space group $Pm\bar{m}n$) are shown.

The final structures were verified for smallness of residual forces, comparison of binding energies of different species, and wave function analyses using an extended triple numerical basis set with two polarization functions per center (TN2P) on a fine grid. Periodic boundary condition calculations were performed in a single Γ -point ($\mathbf{k} = 0$) of the Brillouin zone, which has proved to be a good approximation in previous work on zeolites due to the large size of their unit cells and the wide one-electron band gaps observed (>6 eV at the current level of theory, the experimental value of the optical gap being greater than 9 eV).²⁷

Structural Models. Incorporation of the F^- ion into the silica framework of sodalite was studied using a previously optimized structure of the perfect lattice. The calculated value of the lattice parameter a of the cubic all-silica sodalite (8.878 Å compared to 8.830 Å from a single-crystal X-ray diffraction study of siliceous sodalite that contained ethylene glycol²⁸) was fixed in this study, while full geometry optimization with respect to all internal coordinates was undertaken.

To compensate for the charge of the SiO_4F^- unit, we used a proton that forms a bridging hydroxyl group upon adsorption on the silica framework. The interaction between F^- and H^+ ions strongly distorts the local framework structure, which leads to a number of metastable defect complexes depending on the proximity of the two species.²⁴ Of these defect complexes, only one plausible candidate structure that exhibits a characteristic pentacoordinated Si site with minimal distortion was found for which the separation of the F^- and H^+ based species was at its greatest. The interaction between the F^- and H^+ -based species evidently decreases as the separation distance increases. The total energy of the selected model containing the SiO_4F^- unit is not the lowest of the plausible candidate structures, but it is the only one that contains this unit, for which there is ample experimental XRD and NMR evidence. This system acts mainly as an initial trial to test experimental systems such as the one described below.

Before we discuss the real system that was modeled, we describe the general approach adopted to obtain the true structure of the SiO_4F^- unit in a real system by combining the ab initio computational methods with experimental diffraction techniques. Our approach is summarized in Figure 2. The key steps are as follows: first in step I, we generate an idealized candidate structure based on the geometry resulting from an experimental crystallographic structure solution (A) and perform a periodic ab initio optimization on this structure without any symmetry constraints to yield an optimized true structure with $P1$ symmetry (B). Second, in step II, we apply the symmetry operators of the space group of the experimentally determined structure (A) to each of the atoms in the optimized structure (B) to produce a set of symmetry-related structures from which a set of diffraction intensities is calculated. In this work, we try to model real disorder, in which an experimental diffraction pattern is representative of many slightly different unit cells, by superimposing many slightly different structures into one unit cell. Each of these superimposed structures provides a $1/N$ contribution to the calculated diffraction pattern, where N is the number of structures superimposed into one unit cell. The resulting diffraction intensities are then used to solve and refine a calculated averaged structure (C), which is our prediction, and is subject for comparison with the experimentally derived structure (A). If the two structures are in close agreement, as is the case in our study, the local structure produced in the optimized structure (B) should be considered to be correct. Alternatively, one can determine a calculated average structure directly from the set of symmetry-related structures, from which the set of diffraction intensities was calculated, which is acceptable, but not as rigorous.

To assess the accuracy of the local structure of the SiO_4F^- unit produced in the sodalite system, the same computational procedure was applied to a system based, as closely as possible, on an experimentally determined structure. For this case we took the recently published structure of siliceous ferrierite containing a $[\text{Cu}(\text{pyridine})_2]^{2+}$ complex.¹⁸ The formula of the compound is $\text{Cu}_{0.964}\text{F}_{1.2}(\text{Si}_{36}\text{O}_{72})\cdot 4\text{C}_5\text{H}_5\text{N}$ (A), in which there is one F^- ion site that is bound to only one of the five crystallographically distinct Si atom sites in the framework. The local structural environment is shown in Figure 2(A), and the associated bond lengths and angles within the SiO_4F^- unit are

(27) (a) Sokol, A. A.; Catlow, C. R. A.; Garcés, J. M.; Kuperman, A. *Proceedings 12th International Zeolite Conference*; Treacy, M. M. J., Marcus, B. K., Bisher, M. E., Higgins, J. B., Eds.; Baltimore, 1998. (b) Sokol, A. A.; Catlow, C. R. A.; Garcés, J. M.; Kuperman, A. *J. Phys. Chem. B* **1998**, *102*, 10647.

(28) Richardson, J. W.; Pluth, J. J., Jr.; Smith, J. V.; Dytrych, W. J.; Bibby, D. M. *J. Phys. Chem.* **1988**, *92*, 243.

Table 1. Bond Lengths, Nonbonding Distances (Å), and Bond Angles (deg) for the SiO_4F^- Unit in $\text{Cu}_{0.964}\text{F}_{1.2}(\text{Si}_{36}\text{O}_{72})\cdot 4\text{C}_5\text{H}_5\text{N}$ (A) (Space Group $Pmnn$), $\text{KF}(\text{Si}_{36}\text{O}_{72})\cdot 4\text{C}_5\text{H}_5\text{N}$ (B) (Space Group $P1$), $\text{F}_{1.02(2)}(\text{Si}_{36}\text{O}_{72})$ (C) (Space Group $Pmnn$), and $\text{HF}(\text{Si}_{12}\text{O}_{24})$ (Space Group $P1$) (D)

	A	B	C	D ^a
Si(5)–F(1) (Å)	1.99(2)	1.761	1.990(6)	1.710
Si(5)–O(4)	1.606(3)	1.674	1.629(1)	1.684
Si(5)–O(6)	1.587(4)	1.681	1.608(1)	1.681
Si(5)–O(7)	1.597(3)	1.724	1.620(1)	1.757
Si(5)–O(10)	1.597(3)	1.677	1.622(1)	1.707
F(1)–O(4)	2.17(2)	2.409	2.353(6)	2.393
F(1)–O(6)	1.92(2)	2.380	1.720(6)	2.419
F(1)–O(10)	2.33(2)	2.392	2.311(6)	2.377
O(4)–Si(5)–O(6) (°)	111.2(2)	116.16	108.29(6)	121.57
O(4)–Si(5)–O(7)	105.3(2)	91.12	105.38(6)	90.93
O(4)–Si(5)–O(10)	112.2(2)	123.50	112.60(6)	118.36
O(6)–Si(5)–O(7)	109.7(2)	92.02	112.06(6)	91.82
O(6)–Si(5)–O(10)	110.6(2)	120.05	110.65(6)	120.06
O(7)–Si(5)–O(10)	107.6(2)	92.23	107.79(6)	88.26
O(4)–Si(5)–F(1)	73.3(5)	89.01	80.5(2)	89.69
O(6)–Si(5)–F(1)	64.0(6)	87.45	55.9(2)	91.03
O(7)–Si(5)–F(1)	171.6(6)	179.45	168.0(2)	176.22
O(10)–Si(5)–F(1)	80.4(5)	88.13	78.8(2)	88.17

^a The numbers of the atoms for structure D are used to be consistent with those of A, B, and C but do not correlate to any crystallographic atom assignments given for structural work on sodalite.

given in Table 1. To simplify our modeling system, we replaced the Cu^{2+} cations in the real structure by K^+ cations and changed the occupancy of the K^+ and F^- ion sites so that there was an exact ratio of 1:1 in the structure. The modified formula was now $\text{KF}(\text{Si}_{36}\text{O}_{72})\cdot 4\text{C}_5\text{H}_5\text{N}$. The structure was optimized assuming $P1$ symmetry, and the unit cell parameters were fixed at the values for structure A. The optimized model of $\text{KF}(\text{Si}_{36}\text{O}_{72})\cdot 4\text{C}_5\text{H}_5\text{N}$ in $P1$ symmetry is designated B.

Crystallographic Refinement. The model B discussed above forms the basis for the crystallographic verification to prove that this model can be used to reproduce the experimentally determined structure of the SiO_4F^- unit in A.

From the final optimized structure (B) the K^+ ion and pyridine molecules were removed and the resultant framework structure, with F^- ion still included, was used to produce a single-crystal data set in space group $P1$. Prior to generation of the single-crystal data set, the symmetry operators of space group $Pmnn$ were applied to $\text{F}(\text{Si}_{36}\text{O}_{72})$ (109 atoms) to yield eight structures of $\text{F}(\text{Si}_{36}\text{O}_{72})$ (872 atoms) that were included in the unit cell. To create the same total electron density in the unit cell, each of the 872 atoms was given an occupancy of one-eighth. We would like to reiterate that this procedure was adopted to model real disorder in the system, in which an experimental diffraction pattern is representative of many slightly different unit cells, by superimposing many slightly different structures into one unit cell. The single-crystal data set was produced using the diffraction module of the Catalysis software in the Cerius² suite of programs.²⁹ Polarization, Lorentz, and anomalous dispersion corrections were applied in producing the diffraction intensities, and all the atoms were assumed to have an isotropic temperature factor of 0.022 \AA^2 . The diffraction intensities produced were then used to solve the structure in the space group of the original structure (A), that of $Pmnn$. The structure was solved by direct methods using the program SHELXS-86³⁰ from which all the Si and O atoms were located. The F atom was found from difference Fourier syntheses. The final cycle of least-squares refinement included the atomic positions and anisotropic temperature factors for all atoms and the occupancy of the F atom. The final residuals $R(F)$ and $Rw(F)$ were 2.24% and 1.93%,

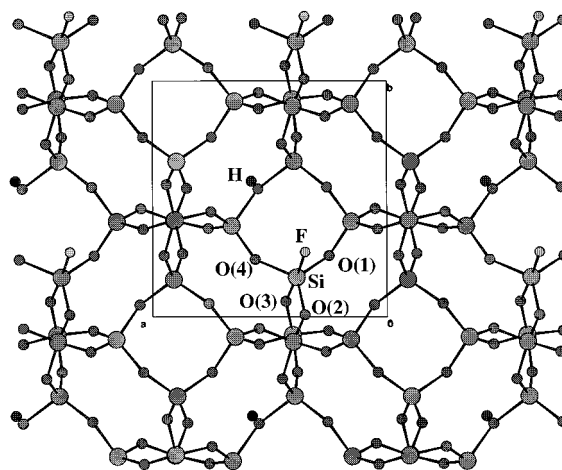


Figure 3. The structure of $\text{HF}(\text{Si}_{12}\text{O}_{24})$ viewed along the $[001]$ direction.

respectively. The bond lengths and angles within the SiO_4F^- unit for the minimized structure in space group $P1$ (B) and the structure of $\text{F}_{1.02(2)}(\text{Si}_{36}\text{O}_{72})$ solved in space group $Pmnn$ (C) are given in Table 1. All data reduction, full matrix-least-squares refinement, and subsidiary calculations were performed using the CRYSTALS suite of programs.³¹

Results and Discussion

Sodalite. The structure of the $\text{HF}(\text{Si}_{12}\text{O}_{24})$ sodalite is shown in Figure 3, where it is seen that the SiO_4F^- unit adopts a regular trigonal bipyramidal structure, for which the bond lengths and angles are given in Table 1. We obtain an Si–F bond length of 1.71 Å, which is considerably shorter than any reported from crystallographic data, but it is closer to those reported for 4-coordinated Si in SiF_4 (1.56 Å) and 6-coordinated Si in SiF_6^{2-} (1.68 Å) molecular units.^{22,23} The larger value we report for the Si–F bond length is understandable as the repulsive interaction of the F^- anion with O^{2-} anions in the SiO_4F^- unit is stronger than with another F^- ion, as found in SiF_4 and SiF_6^{2-} . Moreover, the typical Si–O bond distance for a 4-coordinated Si atom in a zeolite is 1.60 Å. Hence, by adding to a tetrahedral Si site an F^- ion one would expect an increase in the average Si–O,F bond distance. We can also point to an upper-bound estimate, as it is known for the 6-coordinated Si site in stishovite that the Si–O bond distances are 1.76 and 1.81 Å.³² Thus the Si–F bond length we report lies perfectly in the expected range. Another important feature we observe in the SiO_4F^- unit in sodalite is the significant elongation of the Si–O bonds, with particular effect on the Si–O bond (1.76 Å) trans to the Si–F bond. This observation is in accord with the experimentally recovered data,^{8,17} but we also note that the other three Si–O bonds are also elongated, as one would expect for an overcoordinated Si species, which is not easily shown by the experimental crystallographic studies.^{8,17}

We note that the charge separation between H^+ and F^- species in the sodalite framework is fairly small (H^+ – F^- distance of 4.52 Å). The strong character of the Coulomb interaction between the two ions leads to an

(29) Catalysis, Cerius² 3.5, User Guide; Molecular Simulations, Inc.: San Diego, 1997.

(30) Sheldrick G. M. SHELXS-86 Program for Crystal Structure Determination; University of Gottingen: Gottingen, 1986.

(31) Watkin, D. J.; Carruthers, J. R.; Betteridge P. W. CRYSTALS User Guide; Chemical Crystallography Laboratory: Oxford, 1990.

(32) Sinclair, W.; Ringwood, A. E. Nature 1978, 272, 714.

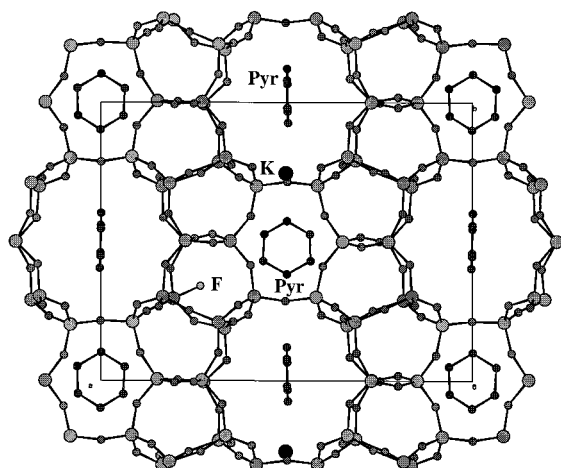


Figure 4. The structure of $\text{KF}(\text{Si}_{36}\text{O}_{72})\cdot 4\text{C}_5\text{H}_5\text{N}$ (B) viewed along the [001] direction. The hydrogen atoms of the pyridine molecules have been omitted for clarity.

appreciable distortion of the flexible framework of the zeolite (Si–O bond lengths in the range 1.57–1.79 Å for the SiO_4 units, as opposed to 1.60 Å for a normal tetrahedral Si), even though the local structure of the SiO_4F^- unit, as seen in the data in Table 1, is largely unaffected.

Ferrierite. The full structural model of the $\text{KF}(\text{Si}_{36}\text{O}_{72})\cdot 4\text{C}_5\text{H}_5\text{N}$ ferrierite (B) is shown in Figure 4. This model retains all the important structural features reported in ref 18, including the location of the extraframework cation and pyridine molecules. The geometry of the latter is in agreement with reported structures.²² The structure of the intact ferrierite framework is reasonable. The Si–O bond length and tetrahedral O–Si–O bond angle ranges in the SiO_4 tetrahedra of B are 1.57–1.66 Å and 101.7–122.3° compared to 1.587–1.603 Å and 106.7–111.5° for A. The slight overestimation of the Si–O bond lengths by ca. 0.03 Å in our calculations is typically obtained using the current level of theory.³³ Otherwise, this model is of high enough precision to base our crystallographic work.

The local structure of the SiO_4F^- unit is shown in Figure 2B, and the corresponding bond lengths and angles are given in Table 1. Again the SiO_4F^- unit adopts a regular trigonal bipyramidal structure, as found in sodalite. The main structural features noted above are also observed for the SiO_4F^- unit in ferrierite, particularly the Si–F bond length of 1.76 Å and the significant elongation of the Si–O bonds, especially for the Si–O_{trans} bond lengths in sodalite (1.71 and 1.76 Å, respectively) and ferrierite (1.76 and 1.72 Å, respectively), which is assumed to be attributable to the different environments of the SiO_4F^- unit in the two materials and is related to factors such as the surrounding Si–O–Si bond angles, whose values are framework dependent and vary between 145° and 180°. The equatorial Si–O bonds in the SiO_4F^- unit in ferrierite are slightly smaller and more regular than in the sodalite, which is in line with the more symmetrical, “intact” character of the calculated ferrierite framework. This

results from a weakened Coulomb interaction between F^- and the counterion (K^+F^- distance of 7.79 Å) supported by the void-filling pyridine molecules.

The values of the geometric parameters given in Table 1 and the structure of the averaged SiO_4F^- unit displayed in Figure 2C show that use of the computationally produced model B of the local structure of the SiO_4F^- unit in the *P1* structure of $\text{KF}(\text{Si}_{36}\text{O}_{72})\cdot 4\text{C}_5\text{H}_5\text{N}$ when refined as $\text{F}_{1.02(2)}(\text{Si}_{36}\text{O}_{72})$ (C) in space group *Pmnn* produces a local structure that is in excellent agreement with the experimentally determined structure of the SiO_4F^- unit in $\text{Cu}_{0.964}\text{F}_{1.2}(\text{Si}_{36}\text{O}_{72})\cdot 4\text{C}_5\text{H}_5\text{N}$ (A) in space group *Pmnn*. The agreement is particularly good for the Si–F bond distances, where values of 1.990(6) and 1.99(2) Å from the refined C and A structures were obtained, respectively. This agreement highlights the fact that the Si–F bond length determined by crystallographic methods is only an average that is longer than the true Si–F distance, which reflects the merging of coherent scattering from seven SiO_4 tetrahedra and one SiO_4F^- trigonal bipyramid per unit cell in this system, which is taken into account in our computational approach.

The position of the F^- ion in structure C has moved closer to O(6) than in structure A. However, such discrepancies are expected as the starting model $\text{KF}(\text{Si}_{36}\text{O}_{72})\cdot 4\text{C}_5\text{H}_5\text{N}$ (B) was not identical to $\text{Cu}_{0.964}\text{F}_{1.2}(\text{Si}_{36}\text{O}_{72})\cdot 4\text{C}_5\text{H}_5\text{N}$ (A) in composition and we are imposing a higher symmetry on the truly *P1* structure of B. This fact is also evident in the larger range of the Si–O bond lengths and O–Si–O bond angles in the SiO_4 units of C (1.608–1.633 Å and 105.06–114.20°, respectively) compared to those in A (1.587–1.603 Å and 106.7–111.5°, respectively) and the fact that the equivalent temperature factors of the atoms in C lie in the range 0.023–0.035 Å², even though they were fixed in the starting *P1* model at 0.022 Å².

Our analysis therefore shows that the predicted geometry for the SiO_4F^- species is fully consistent with the crystallographic data. We also note that the slight discrepancies in the final geometric parameters of C when compared to A arise from the assumptions of the formula of B, the current level of theory of these calculations, and the use of X-ray intensities generated from one structure to represent experimental intensities that are produced in a real system from many slightly differing structures.

Conclusions

This work shows the power of computational methods, in combination with experimental techniques, to determine accurately the structure of units occluded in a solid that, at present, cannot be determined fully from experiment.

The trigonal bipyramidal structure of the SiO_4F^- units we have obtained in sodalite and ferrierite possess similar features. Our calculations show that the experimentally reported structure of the SiO_4F^- unit in ferrierite is not accurate but results from the low occurrence of such units in the material and the fact that only an averaged structure is obtained from crystallographic methods. Our calculations also indicate that the all-silica framework stabilizes negatively charged species by incorporation of the species as part of the framework, as opposed to being an extraframework anion.

(33) Catlow, C. R. A.; Coombes, D. S.; Lewis, D. W.; Pereira, J. C. *G. Chem. Mater.* **1998**, *10*, 3249.

Acknowledgment. We would like to acknowledge M. A. Green, P. Barrett, P. E. Sinclair, J. M. Garces, and A. Kuperman for their useful discussions. M.P.A. would like to thank the Royal Society for the provision of a University Research Fellowship. We also would like to thank EPSRC for funding of the computer facilities and MSI for providing the computational chemistry software used in this work.

Supporting Information Available: Tables of atomic coordinates for HF(Si₁₂O₂₄) and KF(Si₃₆O₇₂)·4C₅H₅N and atomic coordinates, bond lengths and angles, and anisotropic temperature factors for F_{1,02(2)}(Si₃₆O₇₂) are given in CIF format. This material is available free of charge via the Internet at <http://pubs.acs.org>.

CM011141I